NREL
Transforming ENERGY

Towards Advanced Robotics for Wind Blade Manufacturing

Hunter Huth
National Renewable Energy Laboratory
October 2-3, 2024

Photo by Dennis Schroeder, NREL 55200

Presentation Overview

1. Economics of Automated Finishing
2. Tool Design
3. Toolpath Generation
4. Real-Time Control for Automated Finishing
5. Factory Mobility

Offshore wind deployments depend on domestic manufacturing

- To meet 30 gigawatts (GW) by 2030 requires a scenario with no supply chain constraints

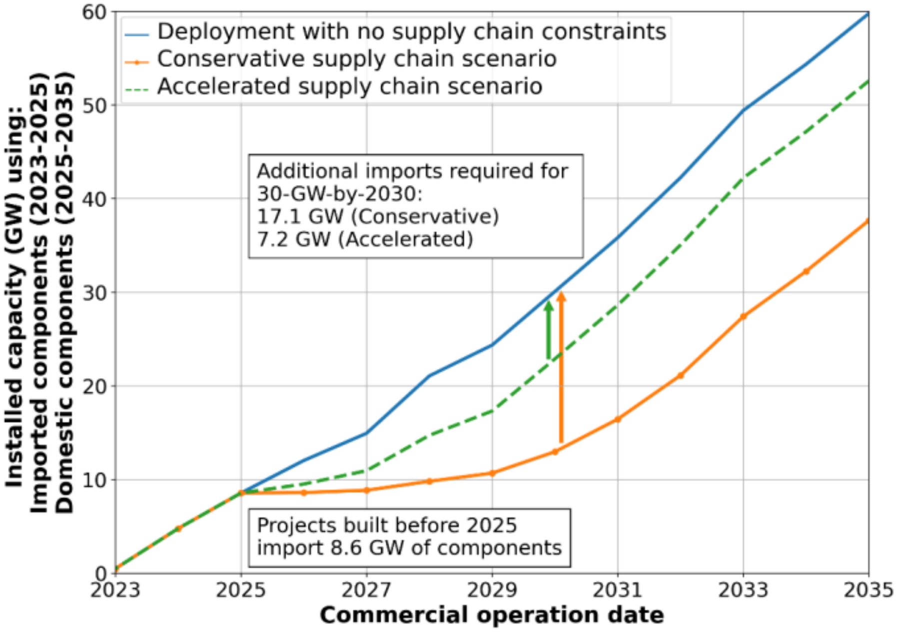

Plot from Shields (2023)

Offshore wind deployments depend on domestic manufacturing

- To meet 30 gigawatts (GW) by 2030 requires a scenario with no supply chain constraints
- This requires five new blade manufacturing facilities to be developed, each producing 225 blades per year

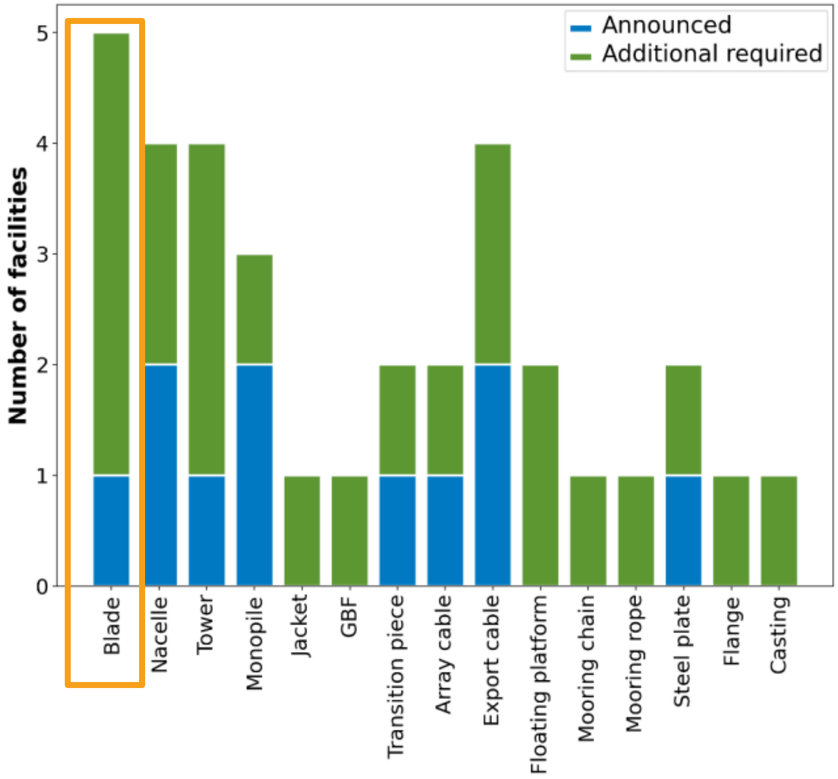

Plot from Shields (2023)

Offshore wind deployments depend on domestic manufacturing

- To meet 30 gigawatts (GW) by 2030 requires a scenario with no supply chain constraints
- This requires five new blade manufacturing facilities to be developed, each producing 225 blades per year
- However, this considers only automation to have an impact in the long term.

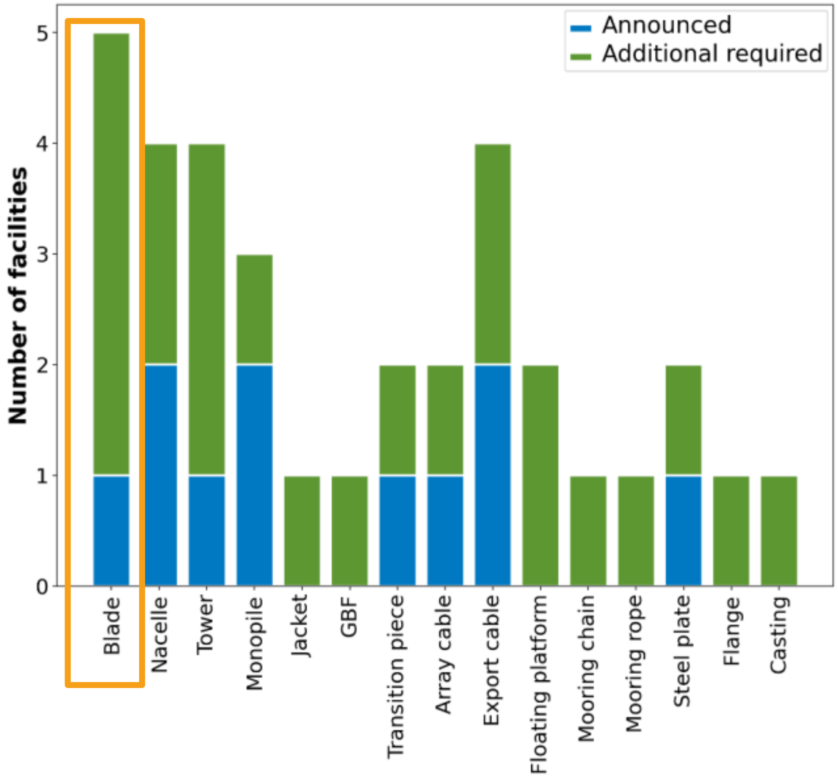

Plot from Shields (2023)

Current breakdown of SNL 100-03 wind turbine blade manufacturing

- Premold steps are difficult to automate
- Automation has a lower material deposition rate
- Automated soft-fabric manipulation has a low technology readiness level.

Operation	Labor [hour]	Skin Mold Gating CT [hour]	Nongating CT [hour]
Material cutting	136.10	[-]	47.57
Root preform lp	16.64	[-]	10.42
Root preform hp	16.64	[-]	10.42
Infusion shear web number 1	155.97	[-]	19.27
Infusion shear web number 2	152.32	[-]	18.91
Infusion shear web number 3	69.18	[-]	10.12
Infusion shear web number 4	24.48	[-]	5.45
Infusion spar cap lp	152.87	[-]	19.51
Infusion spar cap hp	152.87	[-]	19.51
Lp skin	484.73	14.76	[-]
Hp skin	478.77	[-]	14.76
Assembly	443.55	6.33	[-]
Demolding	9.23	2.92	[-]
Trim	23.00	[-]	4.33
Overlay	86.99	[-]	9.91
Postcure	2.17	[-]	9.84
Root cut and drill	14.65	[-]	6.99
Root hardware installation	10.63	[-]	4.98
Surface preparation	145.22	[-]	18.28
Painting	30.82	[-]	7.79
Surface finishing	29.31	[-]	9.83
Weight balance	7.16	[-]	3.25
Final inspection	4.91	[-]	2.04
Shipping preparation	6.21	[-]	2.75
Total	**2,654.46**	**24.00**	**255.93**

Table from Bortolotti (2019)

Current breakdown of SNL 100-03 wind turbine blade manufacturing

- Postmold operations have a much higher technology readiness level and thus make an impact in the short- and mid-term
- Automation can have a huge impact on eliminating supply chain constraints.

Operation	Labor [hour]	Skin Mold Gating CT [hour]	Nongating CT [hour]
Material cutting	136.10	[-]	47.57
Root preform lp	16.64	[-]	10.42
Root preform hp	16.64	[-]	10.42
Infusion shear web number 1	155.97	[-]	19.27
Infusion shear web number 2	152.32	[-]	18.91
Infusion shear web number 3	69.18	[-]	10.12
Infusion shear web number 4	24.48	[-]	5.45
Infusion spar cap lp	152.87	[-]	19.51
Infusion spar cap hp	152.87	[-]	19.51
Lp skin	484.73	14.76	[-]
Hp skin	478.77	[-]	14.76
Assembly	443.55	6.33	[-]
Demolding	9.23	2.92	[-]
Trim	23.00	[-]	4.33
Overlay	86.99	[-]	9.91
Postcure	2.17	[-]	9.84
Root cut and drill	14.65	[-]	6.99
Root hardware installation	10.63	[-]	4.98
Surface preparation	145.22	[-]	18.28
Painting	30.82	[-]	7.79
Surface finishing	29.31	[-]	9.83
Weight balance	7.16	[-]	3.25
Final inspection	4.91	[-]	2.04
Shipping preparation	6.21	[-]	2.75
Total	**2,654.46**	**24.00**	**255.93**

Table from Bortolotti (2019)

Current breakdown of SNL 100-03 wind turbine blade manufacturing

- Trimming removes excess flashing material
  - Uses a cutting tool to remove the bulk of material
  - Grinds the remaining material to produce an aerodynamic shape

Operation	Labor [hour]	Skin Mold Gating CT [hour]	Nongating CT [hour]
Material cutting	136.10	[-]	47.57
Root preform lp	16.64	[-]	10.42
Root preform hp	16.64	[-]	10.42
Infusion shear web number 1	155.97	[-]	19.27
Infusion shear web number 2	152.32	[-]	18.91
Infusion shear web number 3	69.18	[-]	10.12
Infusion shear web number 4	24.48	[-]	5.45
Infusion spar cap lp	152.87	[-]	19.51
Infusion spar cap hp	152.87	[-]	19.51
Lp skin	484.73	14.76	[-]
Hp skin	478.77	[-]	14.76
Assembly	443.55	6.33	[-]
Demolding	9.23	2.92	[-]
Trim	23.00	[-]	4.33
Overlay	86.99	[-]	9.91
Postcure	2.17	[-]	9.84
Root cut and drill	14.65	[-]	6.99
Root hardware installation	10.63	[-]	4.98
Surface preparation	145.22	[-]	18.28
Painting	30.82	[-]	7.79
Surface finishing	29.31	[-]	9.83
Weight balance	7.16	[-]	3.25
Final inspection	4.91	[-]	2.04
Shipping preparation	6.21	[-]	2.75
Total	**2,654.46**	**24.00**	**255.93**

Table from Bortolotti (2019)

Current breakdown of SNL 100-03 wind turbine blade manufacturing

- Trimming removes excess flashing material
  - Uses a cutting tool to remove the bulk of material
  - Grinds the remaining material to produce an aerodynamic shape
- Surface preparation is done before painting and adding protective coating.

Operation	Labor [hour]	Skin Mold Gating CT [hour]	Nongating CT [hour]
Material cutting	136.10	[-]	47.57
Root preform lp	16.64	[-]	10.42
Root preform hp	16.64	[-]	10.42
Infusion shear web number 1	155.97	[-]	19.27
Infusion shear web number 2	152.32	[-]	18.91
Infusion shear web number 3	69.18	[-]	10.12
Infusion shear web number 4	24.48	[-]	5.45
Infusion spar cap lp	152.87	[-]	19.51
Infusion spar cap hp	152.87	[-]	19.51
Lp skin	484.73	14.76	[-]
Hp skin	478.77	[-]	14.76
Assembly	443.55	6.33	[-]
Demolding	9.23	2.92	[-]
Trim	23.00	[-]	4.33
Overlay	86.99	[-]	9.91
Postcure	2.17	[-]	9.84
Root cut and drill	14.65	[-]	6.99
Root hardware installation	10.63	[-]	4.98
Surface preparation	145.22	[-]	18.28
Painting	30.82	[-]	7.79
Surface finishing	29.31	[-]	9.83
Weight balance	7.16	[-]	3.25
Final inspection	4.91	[-]	2.04
Shipping preparation	6.21	[-]	2.75
Total	**2,654.46**	**24.00**	**255.93**

Table from Bortolotti (2019)

Due to high labor costs, automation can encourage manufacturers to locate in the United States

- Automated finishing can
  - Increase quality
  - Reduce cycle time
  - Increase throughput

Due to high labor costs, automation can encourage manufacturers to locate in the United States

- Automated finishing can
  - Increase quality
  - Reduce cycle time
  - Increase throughput
- However, to make automated wind turbine blade finishing economically viable:
  - Keep capital costs low
  - Be able to adapt to new blade designs
  - Dramatically reduce cycle time.

Our techno-economic model shows that an ~62% reduction in finishing time is needed

- If capital costs are spread over 3 years, an ~60% reduction in finishing costs per blade is achieved

Our techno-economic model shows that an ~62% reduction in finishing time is needed

- If capital costs are spread over 3 years, an ~60% reduction in finishing costs per blade is achieved
- Using the SNL 100-03 reference blade (Bortolotti 2019):
  - 10 meters (m) per hour (hr) per worker for 6 workers = 1 m per minute (min)
    - Automated trimming speed of 1.62 m/min

Our techno-economic model shows that an ~62% reduction in finishing time is needed

- If capital costs are spread over 3 years, an ~60% reduction in finishing costs per blade is achieved
- Using the SNL 100-03 reference blade (Bortolotti 2019):
  – 10 meters (m) per hour (hr) per worker for 6 workers = 1 m per minute (min)
    - Automated trimming speed of 1.62 m/min
  – 6 m^2/worker/hr for 8 workers = .8 m^2/min
    - Automated sanding speed of 1.296 m^2/min.

Tool Design for Automated Wind Turbine Blade Finishing

Phase 1

Robots can use more aggressive tooling

- Robots can carry heavy payloads, produce high forces, and move quickly
- KUKA KR300 R2500 Ultra (2021), with a linear track, has the following features:
  - 2.5-m reach, 300-kilogram (kg) payload, 6.6-m track
  - Can reach up to 2.5 m per second (s).

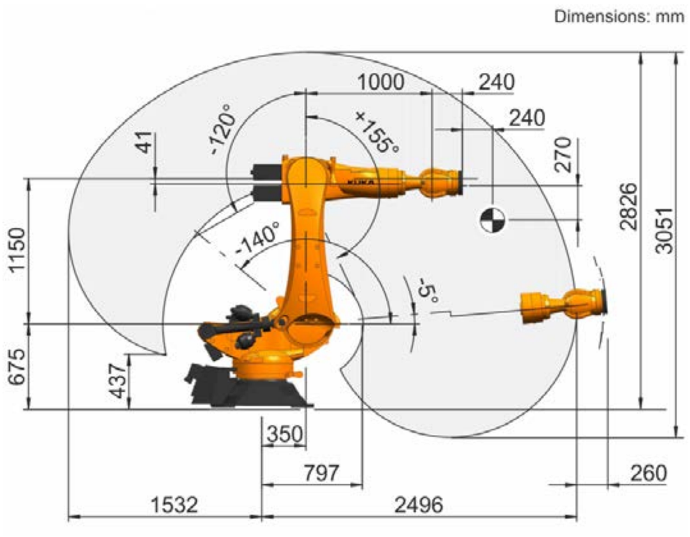

Photo from KUKA KR300 R2500

Trimming tool selection

- Band saw modified for cutting the bulk of flashing material from the wind turbine blade

Photo by Hunter Huth, NREL

Trimming tool selection

- Band saw modified for cutting the bulk of flashing material from the wind turbine blade
- Diamond band-saw blades provide superior longevity

Photo by Hunter Huth, NREL

Trimming tool selection

- Band saw modified for cutting the bulk of flashing material from the wind turbine blade
- Diamond band-saw blades provide superior longevity
- Much faster trimming speeds compared to hand-held tools

Photo by Hunter Huth, NREL

Trimming tool selection

- Band saw modified for cutting the bulk of flashing material from the wind turbine blade
- Diamond band-saw blades provide superior longevity
- Much faster trimming speeds compared to hand-held tools
- Equipped with rpm and motor load sensors to adjust speed based on resistance.

Photo by Hunter Huth, NREL

Grinding tool selection

- PushCorp (2020) AFD1240 active compliance device with STC1515 spindle

Photo by Hunter Huth, NREL

Grinding tool selection

- PushCorp (2020) AFD1240 active compliance device with STC1515 spindle
- Custom dust collection shroud

Photo by Hunter Huth, NREL

Grinding tool selection

- PushCorp (2020) AFD1240 active compliance device with STC1515 spindle
- Custom dust collection shroud
- Flapped sanding wheels for more abrasive longevity

Photo by Hunter Huth, NREL

Grinding tool selection

- PushCorp (2020) AFD1240 active compliance device with STC1515 spindle
- Custom dust collection shroud
- Flapped sanding wheels for longevity
- Allows precise force control to consistently remove the desired amount of material.

Photo by Hunter Huth, NREL

Sanding tool selection

- Tyrolit (2024) drum sander on the PushCorp active compliance device

Photo by Hunter Huth, NREL

Sanding tool selection

- Tyrolit (2024) drum sander on the PushCorp active compliance device
- Allows application of consistent force with constantly changing orientation

Photo by Hunter Huth, NREL

Sanding tool selection

- Tyrolit (2024) drum sander on the PushCorp active compliance device
- Allows application of consistent force with constantly changing orientation
- Drum sanders do not trap dust under the abrasive, resulting in more efficient use.

Photo by Hunter Huth, NREL

Toolpath Generation For Automated Finishing (2024)

Phase 2

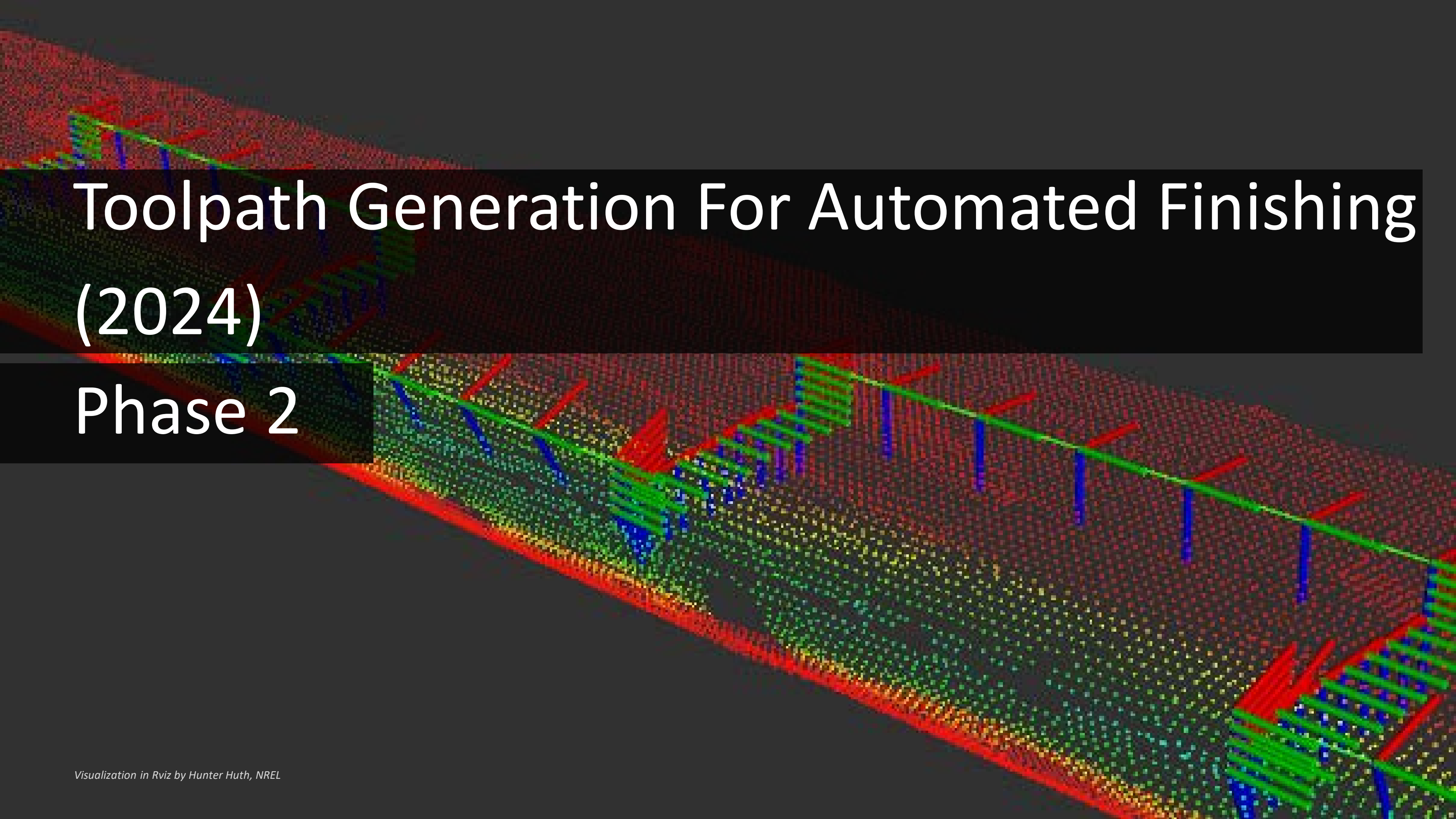

Visualization in Rviz by Hunter Huth, NREL

Capturing blade geometry is a two-step process

- A global scan captures 3D point cloud data of the entire scene
- Blade position is determined by scene segmentation
- A local scan of the leading/trailing edge at the optimal distance for the Zivid 2 camera (2023) is performed.

4× speed

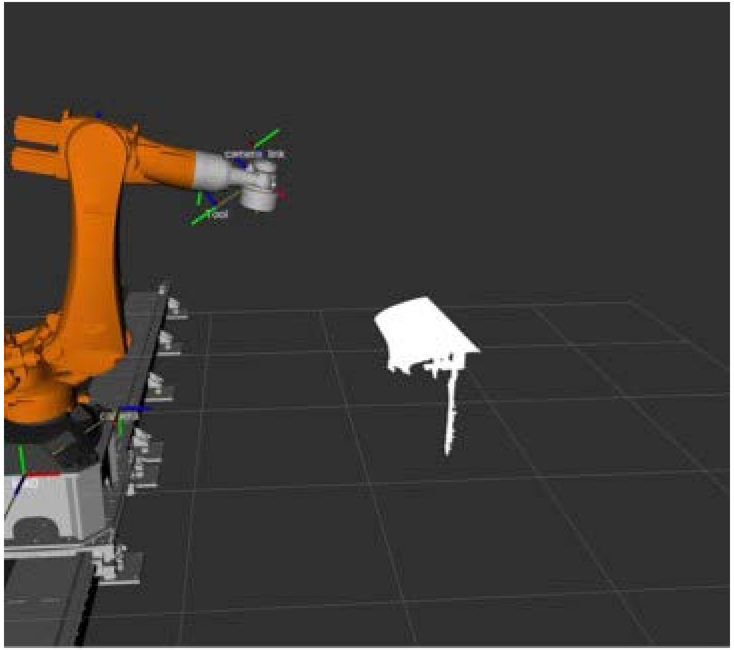

Screen record of Rviz by Hunter Huth, NREL

First step is to identify important geometry on the wind turbine blade

- A moving least squares implemented through the point cloud library (Rusu, 2011) is used to fit a smooth surface to the blade

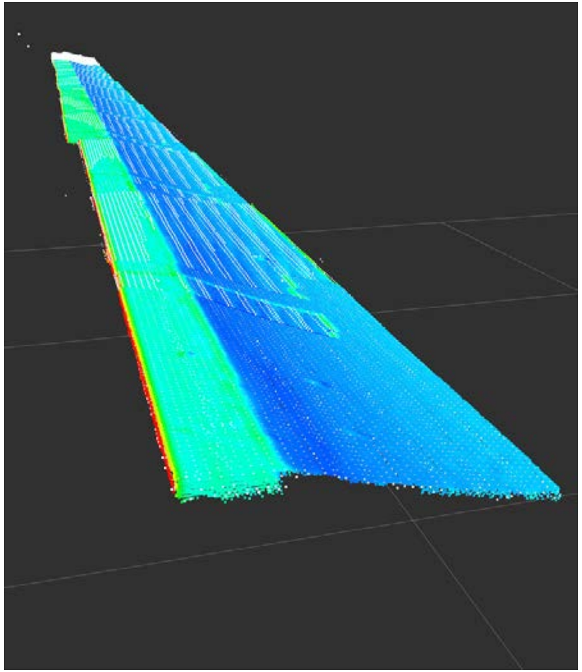

Screen capture of Rviz by Hunter Huth, NREL

First step is to identify important geometry on the wind turbine blade

- A moving least squares implemented through the point cloud library (Rusu 2011) is used to fit a smooth surface to the blade
- The cloud is sliced in the spanwise direction

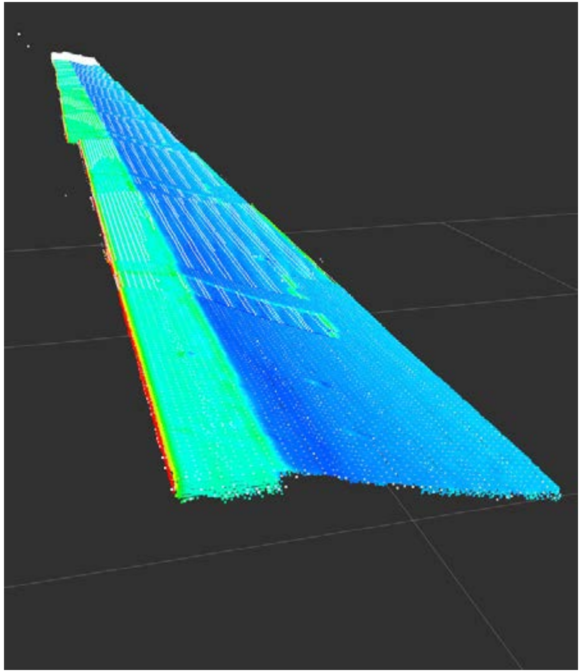

Screen capture of Rviz by Hunter Huth, NREL

First step is to identify important geometry on the wind turbine blade

- A moving least squares implemented through the point cloud library (PCL 2011) is used to fit a smooth surface to the blade
- The cloud is sliced in the spanwise direction
- Normal vectors in the chordwise direction are calculated and analyzed to find large changes in the normal at the leading edge/flashing boundary.

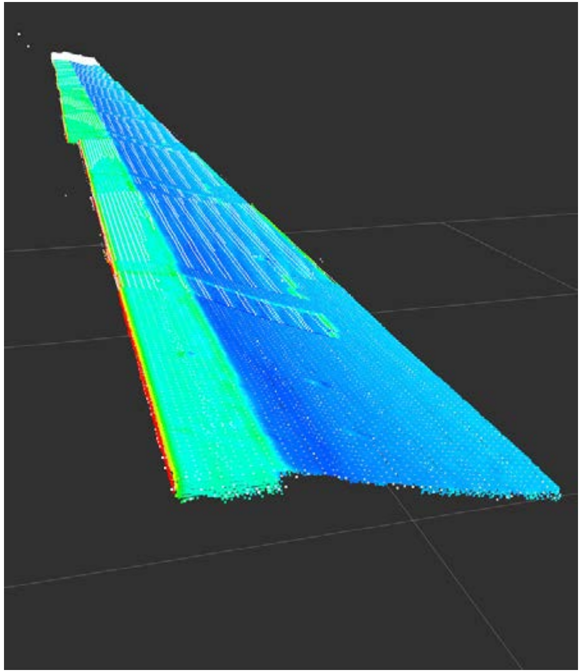

Screen capture of Rviz by Hunter Huth, NREL

Trimming toolpath generation

- Normal components in chordwise direction are calculated along the chord shown in the top plot

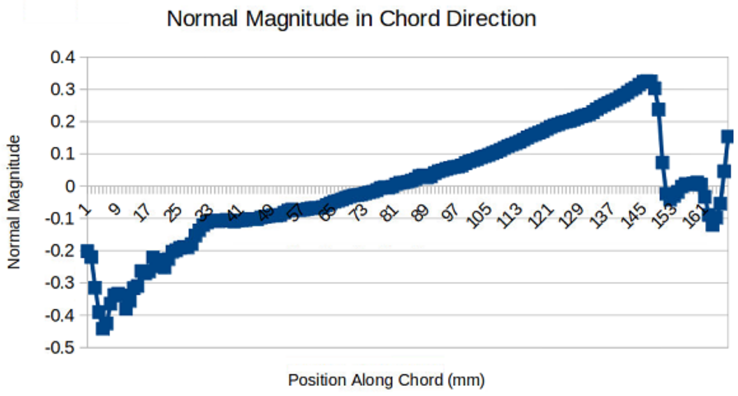

Plots by Hunter Huth

Trimming toolpath generation

- Normal components in chordwise direction are calculated along the chord shown in the top plot
- Difference between adjacent normal vector magnitudes is calculated along the chord shown in the bottom plot
  - Analogous to first derivative

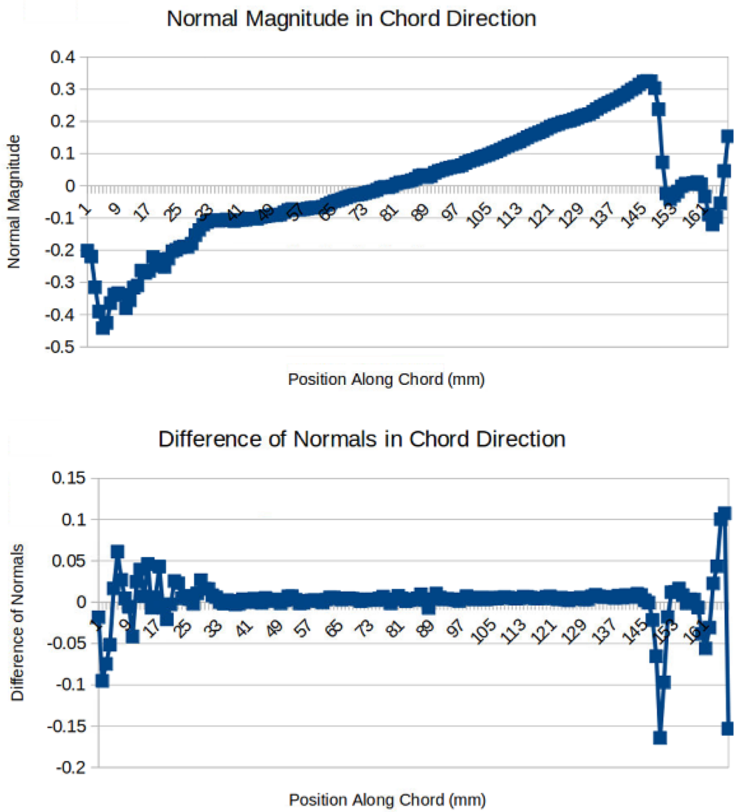

Plots by Hunter Huth

Trimming toolpath generation

- Normal components in chordwise direction are calculated along the chord shown in the top plot
- Difference between adjacent normal vector magnitudes is calculated along the chord shown in the bottom plot
  – Analogous to first derivative
- Flashing begins at the horizontal line, discovered by reducing high-frequency noise and finding the absolute maximum.

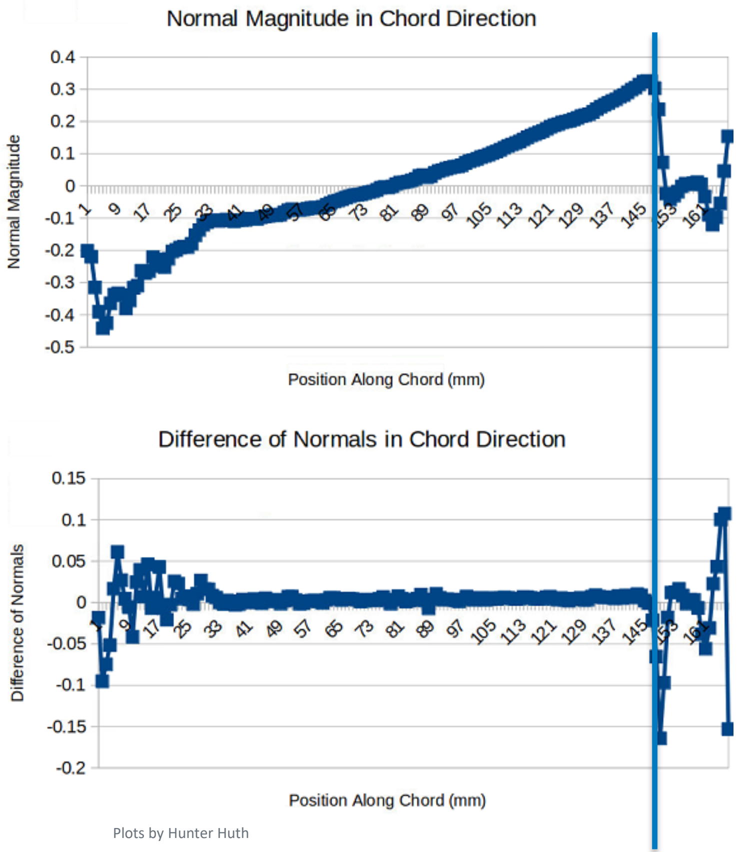

Plots by Hunter Huth

Trimming toolpath calculated from the leading/trailing edge

- An offset is added to prevent damage to the blade

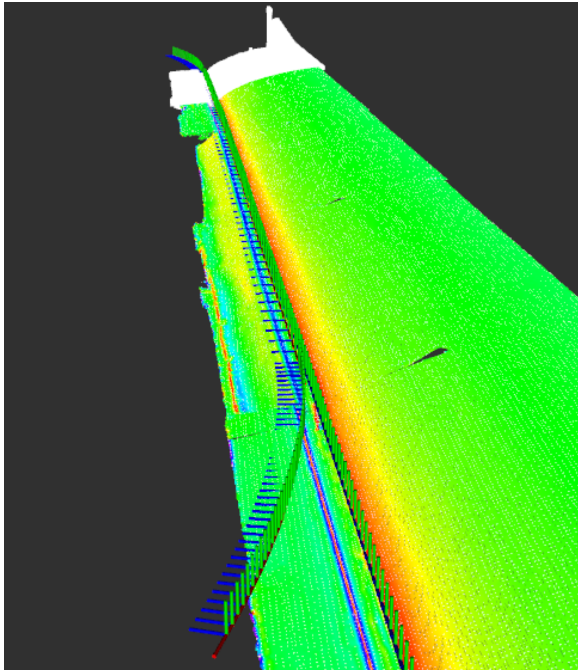

Screen capture of Rviz by Hunter Huth, NREL

Trimming toolpath calculated from the leading/trailing edge

- An offset is added to prevent damage to the blade
- Lead-ins and lead-outs are added every 2.5 meters to separate hanging flashings

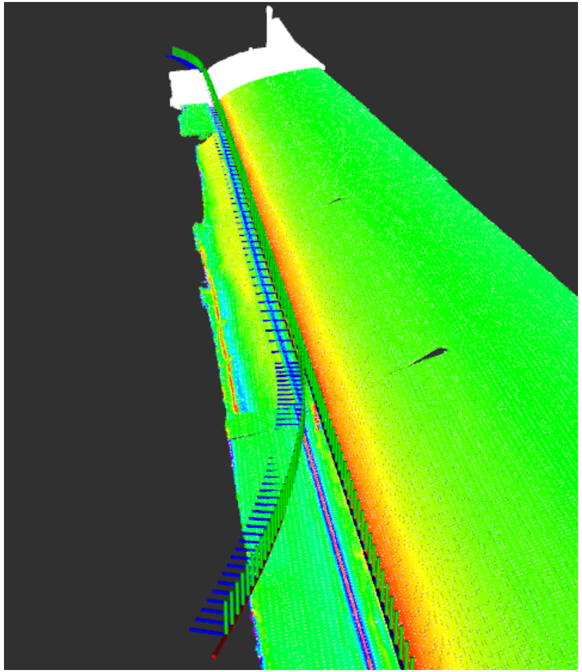

Screen capture of Rviz by Hunter Huth, NREL

Trimming toolpath calculated from the leading/trailing edge

- An offset is added to prevent damage to the blade
- Lead-ins and lead-outs are added every 2.5 meters to separate hanging flashings
- This toolpath is passed as a spline trajectory to the robot controller.

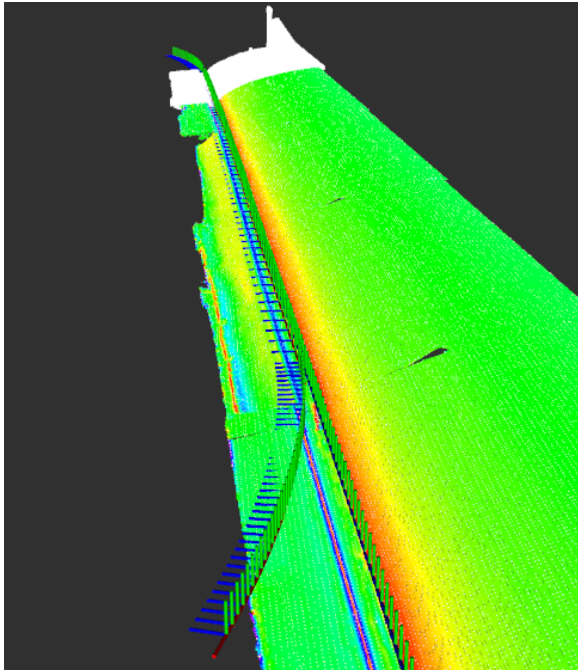

Screen capture of Rviz by Hunter Huth, NREL

Trimming execution

Leading Edge—4× speed

Trailing Edge—4× speed

Videos by Hunter Huth, NREL

Identifying leftover nose material after trimming from point cloud

- Slice leading-edge area into 2D cross sections

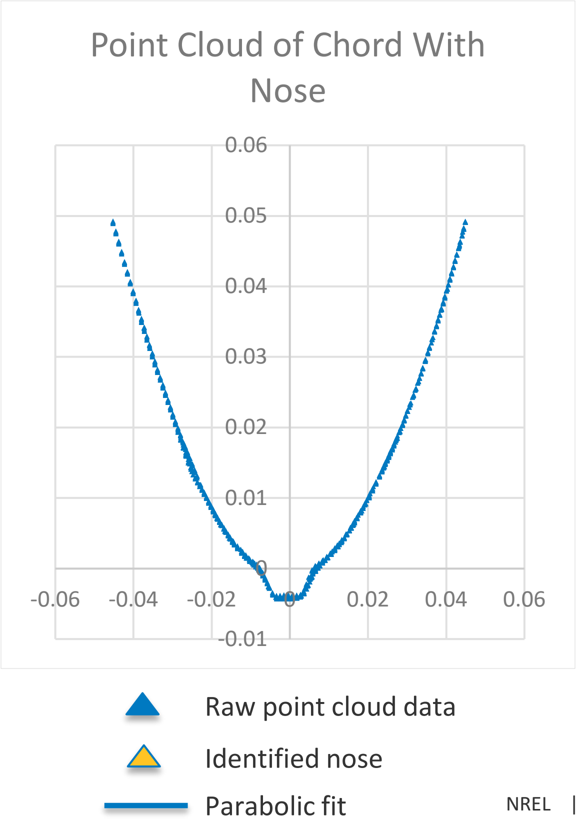

Plots by Hunter Huth

Identifying leftover nose material after trimming from point cloud

- Slice leading-edge area into 2D cross sections
- Fit a parabola along the leading-edge chord

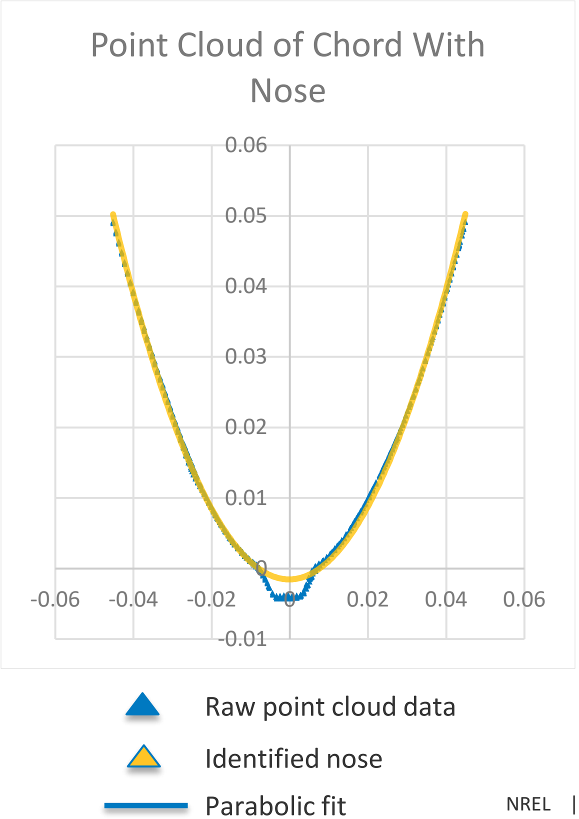

Plots by Hunter Huth

Identifying leftover nose material after trimming from point cloud

- Slice leading-edge area into 2D cross sections
- Fit a parabola along the leading-edge chord
- Use parabola minimum as leading edge

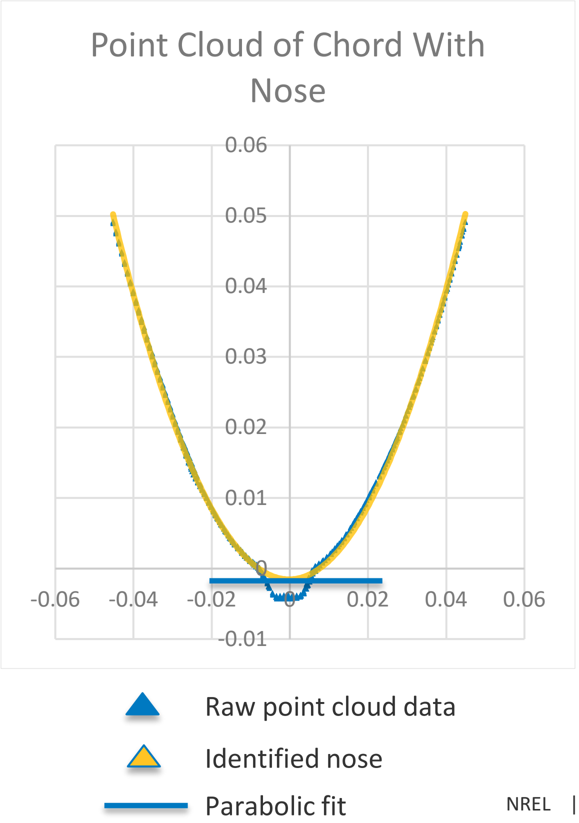

Plots by Hunter Huth

Identifying leftover nose material after trimming from point cloud

- Slice leading-edge area into 2D cross sections
- Fit a parabola along the leading-edge chord
- Use parabola minimum as leading edge
- Extract nose points below parabola minimum

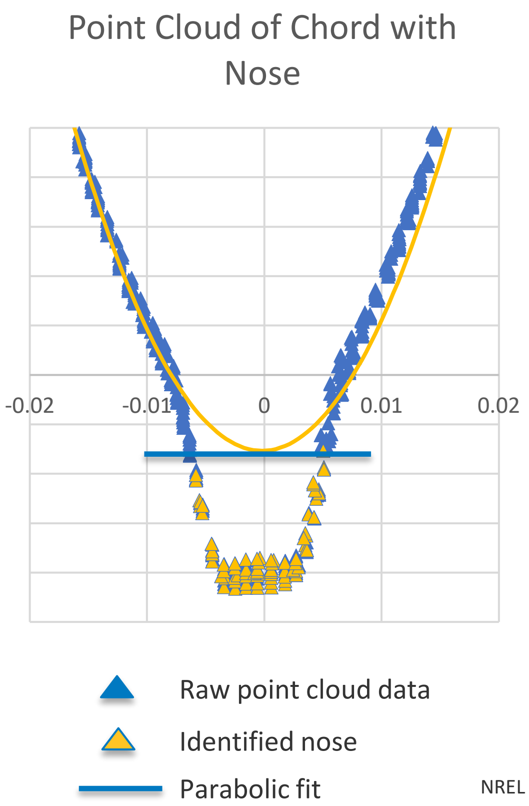

Identifying leftover nose material after trimming from point cloud

- Slice leading-edge area into 2D cross sections
- Fit a parabola along the leading-edge chord
- Use parabola minimum as leading edge
- Extract nose points below parabola minimum
- Nose thickness (N_t) is the average y-distance to the leading edge
- Nose width (N_w) is the range of nose points in the x-direction.

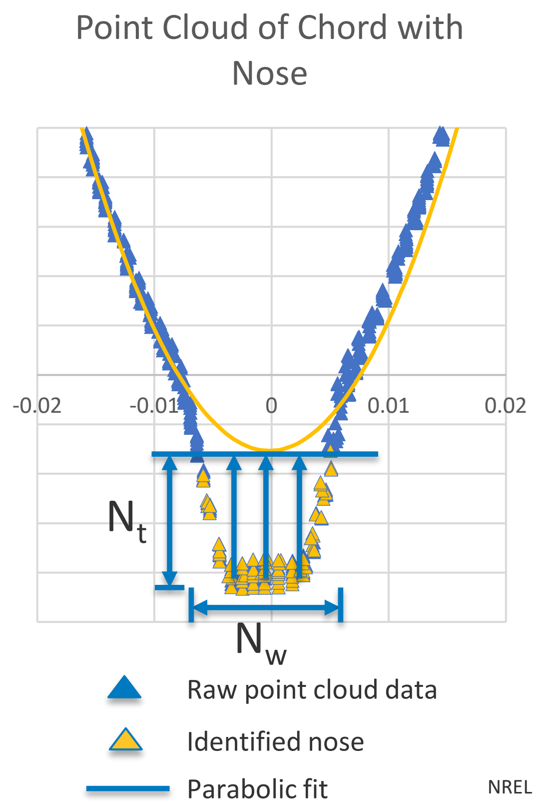

Plots by Hunter Huth

Grinding model for calculating travel velocity

- Model determines linear travel speed necessary to grind to a certain depth
- On first contact, pressure is high, so grinding depth increases
- Pressure decreases as grinder plunges into material until a steady-state depth is reached.

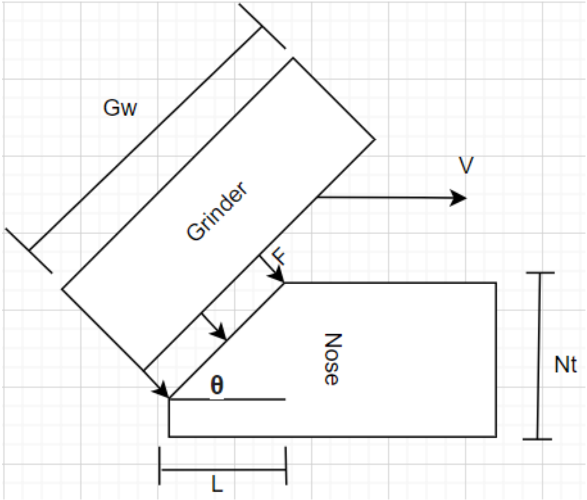

G_w = grinder width
F = force
V = linear velocity
Θ = grinding angle
L = contact length
N_t = nose thickness
N_w = nose width
t = grind time
μ = removal constant

Image by Hunter Huth

Grinding model for calculating travel velocity

$$L = \frac{\mathrm{N_t}}{\tan(\theta)}, \qquad t = \frac{L}{V} = \frac{\mathrm{N_t}}{R} = \frac{\mathrm{N_t}}{\tan(\theta) * V}$$

Time each slice is in contact with grinder

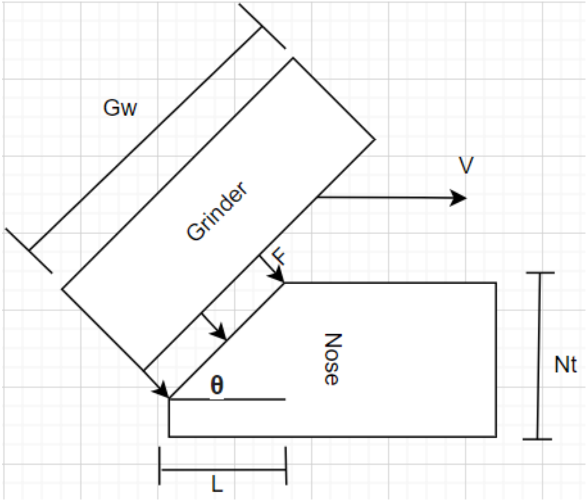

G_w = grinder width
F = force
V = linear velocity
Θ = grinding angle
L = contact length
N_t = nose thickness
N_w = nose width
t = grind time
μ = removal constant

Image by Hunter Huth

Grinding model for calculating travel velocity

$$L = \frac{N_t}{\tan(\theta)}, \qquad t = \frac{L}{V} = \frac{N_t}{R} = \frac{N_t}{\tan(\theta) * V}$$

Time each slice is in contact with grinder

$$V = \frac{R}{\tan(\theta)}, \qquad \boxed{R = \frac{F}{A} * \mu,} \qquad A = N_w * N_t * \sin(\theta)$$

Rate at which material is removed

Contact area of grinder and nose

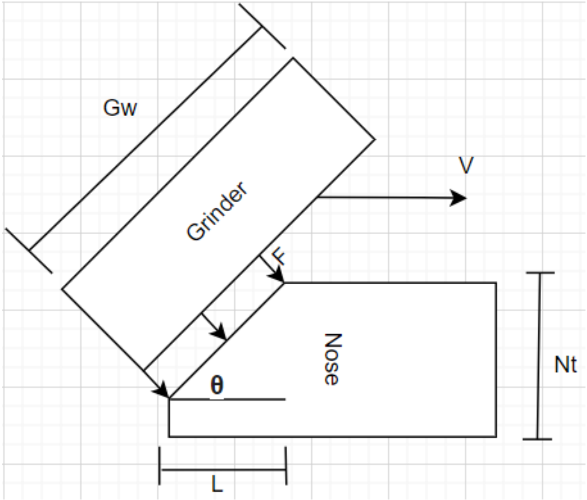

G_w = grinder width

F = force

V = linear velocity

Θ = grinding angle

L = contact length

N_t = nose thickness

N_w = nose width

t = grind time

μ = removal constant

Image by Hunter Huth

Grinding model for calculating travel velocity

$$L = \frac{N_t}{\tan(\theta)}, \qquad t = \frac{L}{V} = \frac{N_t}{R} = \frac{N_t}{\tan(\theta) * V}$$

Time each slice is in contact with grinder

$$V = \frac{R}{\tan(\theta)}, \qquad \boxed{R = \frac{F}{A} * \mu,} \qquad A = N_w * N_t * \sin(\theta)$$

Rate at which material is removed

Contact area of grinder and nose

$$\boxed{V = \frac{F * \mu * \cos(\theta)}{N_w * N_t}}$$

μ characterizes relationship between pressure and removal rate

Linear velocity to remove nose given a grinding angle, force, nose size, and removal constant

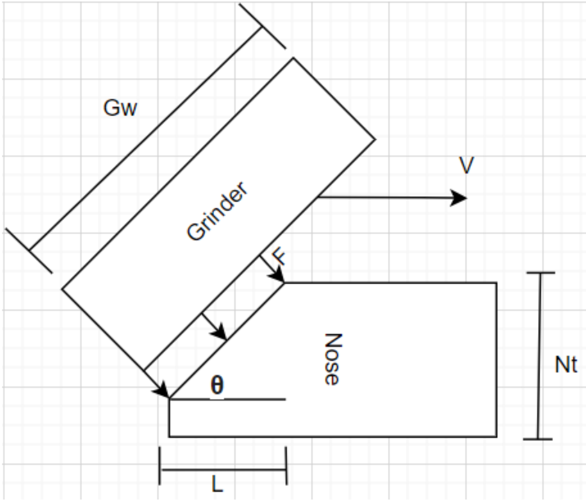

G_w = *grinder width*
F = *force*
V = *linear velocity*
Θ = *grinding angle*
L = *contact length*
N_t = *nose thickness*
N_w = *nose width*
t = *grind time*
μ = *removal constant*

Image by Hunter Huth

Grinding toolpath executed in multiple passes

- Maximum material removed per pass is 2 millimeters (mm)
- The pass length is optimized for longer passes to get a smooth finish.

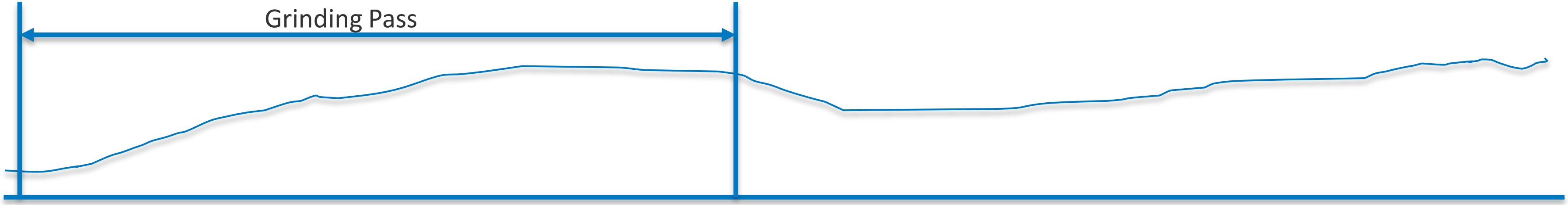

N_t	2	4	6	7	8	7	5	5	7	8	9
Pass 1	0	2	4	5	6	6	5	5	7	8	9
Pass 2											
Pass 3											

Small N_t has only 1 mm removed

End grinding pass because N_t is smaller than previous max N_t

Grinding toolpath executed in multiple passes

- Maximum material removed per pass is 2 millimeters (mm)
- The pass length is optimized for longer passes to get a smooth finish.

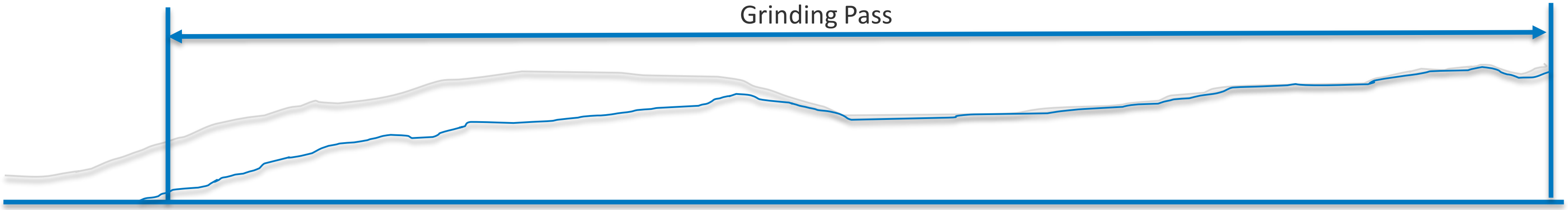

N_t	2	4	6	7	8	7	5	5	7	8	9
Pass 1	0	2	4	5	6	6	5	5	7	8	9
Pass 2	0	0	2	3	4	4	4	4	5	6	7
Pass 3											

Small N_t has only 1 mm removed

Grinding toolpath executed in multiple passes

- Maximum material removed per pass is 2 millimeters (mm)
- The pass length is optimized for longer passes to get a smooth finish.

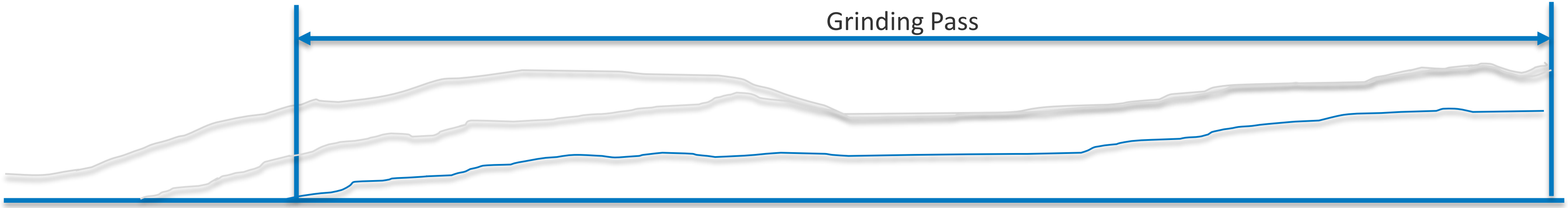

N_t	2	4	6	7	8	7	5	5	7	8	9
Pass 1	0	2	4	5	6	6	5	5	7	8	9
Pass 2	0	0	2	3	4	4	4	4	5	6	7
Pass 3	0	0	0	1	2	2	2	2	3	4	5

Leading- and trailing-edge detection for sanding toolpath

- Leading edge is detected through same algorithm as in the grinding process

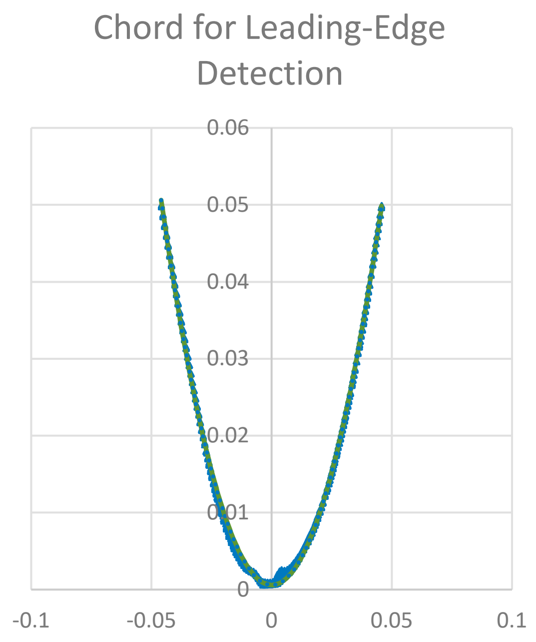

Plot by Hunter Huth

Leading- and trailing-edge detection for sanding toolpath

- Leading edge is detected through same algorithm as in the grinding process
- Trailing edge for sanding is detected with the same algorithm as for trailing-edge trimming
  - Needs scans above and below trailing edge
  - Large change in normal at trailing edge.

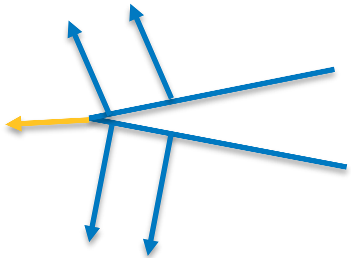

Image by Hunter Huth

Leading-edge sanding toolpath generation

- Separate leading-edge chords into sections that match width of sanding drum

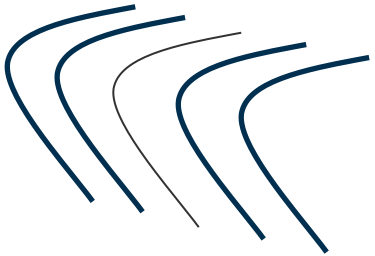

Drawing created by Hunter Huth, NREL

Leading-edge sanding toolpath generation

- Separate leading-edge chords into sections that match width of sanding drum
- Toolpath position follows the middle of the chord

Drawing created by Hunter Huth, NREL

Leading-edge sanding toolpath generation

- Separate leading-edge chords into sections that match width of sanding drum
- Toolpath position follows the middle of the chord
- Toolpath orientation is the average orientation along the chords

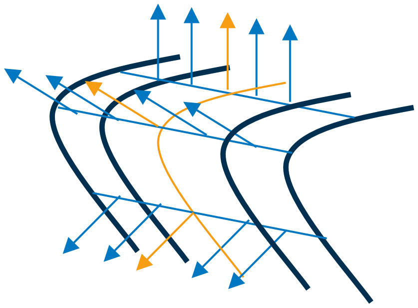

Drawing created by Hunter Huth, NREL

Leading-edge sanding toolpath generation

- Separate leading-edge chords into sections that match width of sanding drum
- Toolpath position follows the middle of the chord
- Toolpath orientation is the average orientation along the chords
- Add lead-in/lead-outs for a soft touch with the sander

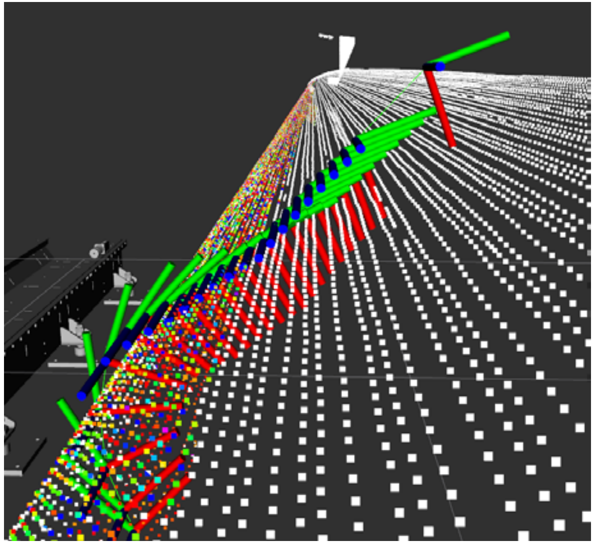

Screen capture of Rviz by Hunter Huth, NREL

Trailing-edge sanding toolpath generation

- Trailing-edge sanding toolpath follows the spanwise direction
- Sander angle relative to the trailing edge is calculated to sand to the desired chord depth and optimize abrasive usage

Photo by Hunter Huth, NREL

Trailing-edge sanding toolpath generation

- Trailing-edge sanding toolpath follows the spanwise direction
- Sander angle relative to the trailing edge is calculated to sand to the desired chord depth and optimize abrasive usage
- Sander orientation is determined by the average normal orientation under the sanding drum.

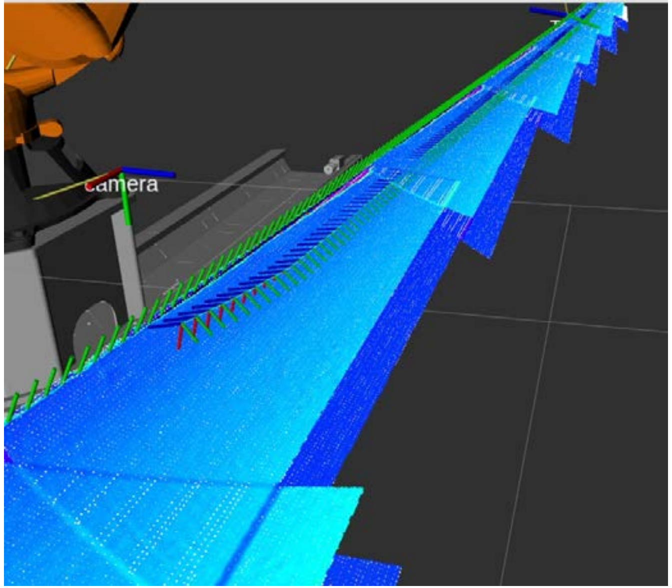

Screen capture of Rviz by Hunter Huth, NREL

Sanding execution

Leading Edge—4× speed

Trailing Edge—4× speed

Videos by Hunter Huth, NREL

Automated finishing results

- Trimming accuracy of -4.5/+0.7 mm and -3.1/+3.6 mm for leading and trailing edge, respectively

	Operational Speed (m/min)	
	Leading Edge	Trailing Edge
Trim	0.96	1.09
Grind	0.63	N/A
Sand	0.79	0.81

Automated finishing results

- Trimming accuracy of -4.5/+0.7 mm and -3.1/+3.6 mm for leading and trailing edge, respectively
- Grinding could not consistently remove the correct amount of material
  - Real-time feedback required to update the grinding model

	Operational Speed (m/min)	
	Leading Edge	Trailing Edge
Trim	0.96	1.09
Grind	0.63	N/A
Sand	0.79	0.81

Automated finishing results

- Trimming accuracy of -4.5/+0.7 mm and -3.1/+3.6 mm for leading and trailing edge, respectively
- Grinding could not consistently remove the correct amount of material
  - Real-time feedback required to update the grinding model
- Sanding offered full and even coverage of the surface.

	Operational Speed (m/min)	
	Leading Edge	Trailing Edge
Trim	0.96	1.09
Grind	0.63	N/A
Sand	0.79	0.81

Real-Time Control

Phase 3

Image By Hunter Huth, NREL

Real-time control to optimize for speed and accuracy

- Previous phase focused on how to use captured blade geometry to plan toolpaths

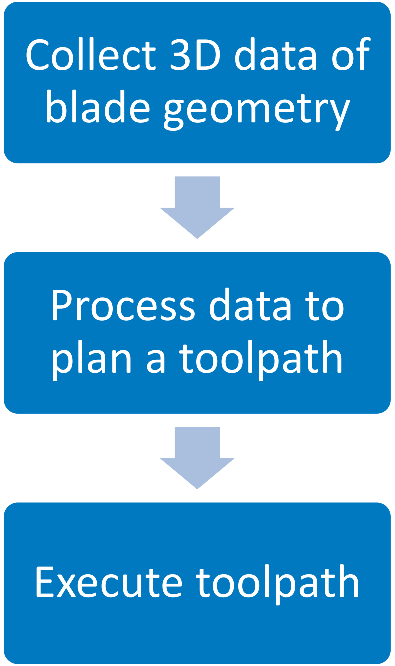

Real-time control to optimize for speed and accuracy

- Previous phase focused on how to use captured blade geometry to plan toolpaths
- Sequentially captured data, planned a toolpath, and executed the toolpath
  - Inefficient in terms of cycle time

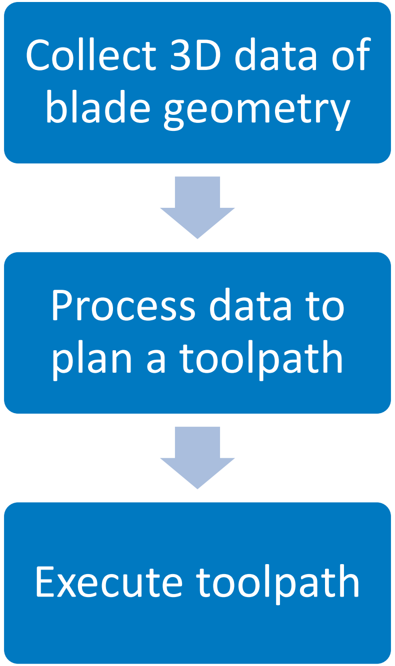

Real-time control to optimize for speed and accuracy

- Previous phase focused on how to use captured blade geometry to plan toolpaths
- Sequentially captured data, planned a toolpath, and executed the toolpath
  - Inefficient in terms of cycle time
- Next phase will scan, plan, and execute in parallel
  - Substantial reduction in cycle time
  - Limited by tool operation speed
  - Real-time feedback to improve finish quality.

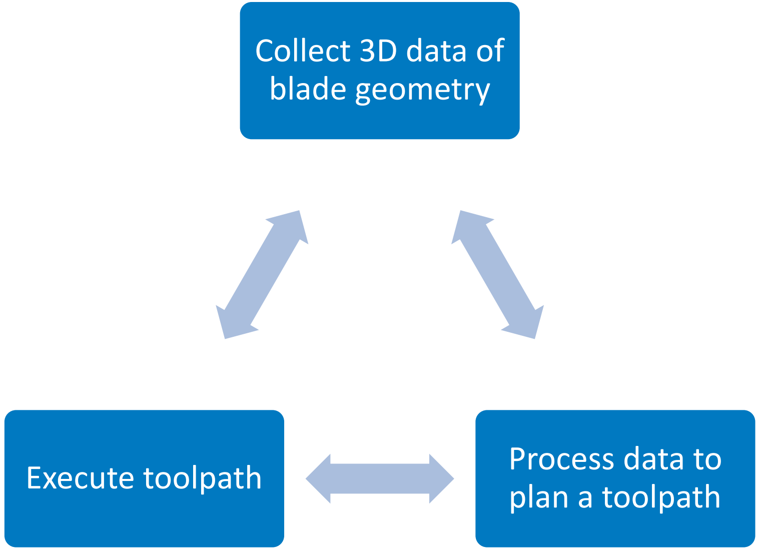

Real-time control of an industrial robot

- Kuka has a real-time interface that allows streaming of joint commands every 4 milliseconds (ms)
  - Allows finite control of joints to improve accuracy

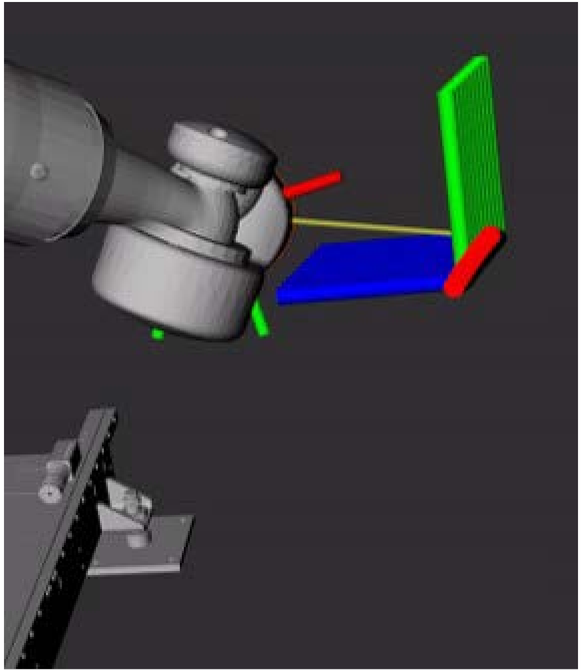

Image by Hunter Huth, NREL

Real-time control of an industrial robot

- Kuka has a real-time interface that allows streaming of joint commands every 4 milliseconds (ms)
  - Allows finite control of joints to improve accuracy
- Trajectory will be planned from Robot Operating System (ROS) 2 (Macenski, 2022)
  - Real-time improvements from ROS that leverage a real-time kernel.

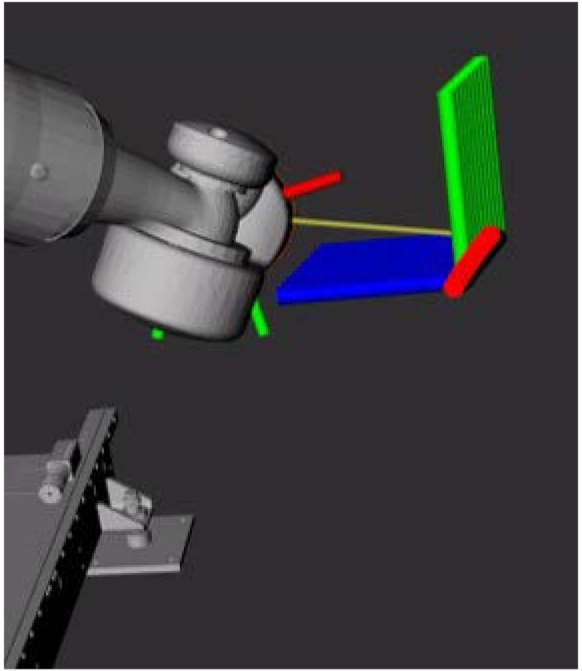

Image by Hunter Huth, NREL

Capture data with a 3D laser line profiler

- Capture real-time scans in the chordwise direction
  - Faster processing of chords
  - Capture and process data while performing the operation
- Real-time quality feedback to ensure the correct aerodynamic shape is being produced.

Photo by Casey Nichols, NREL

How does this robot reach the entire surface?

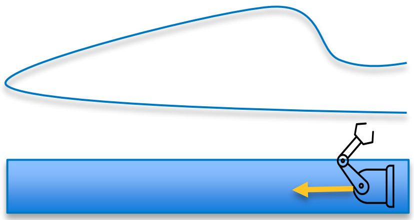

Full-Length Track With Stationary Blade

+Requires less factory space
+Simple concept
−High track cost
−Less flexibility

How does this robot reach the entire surface?

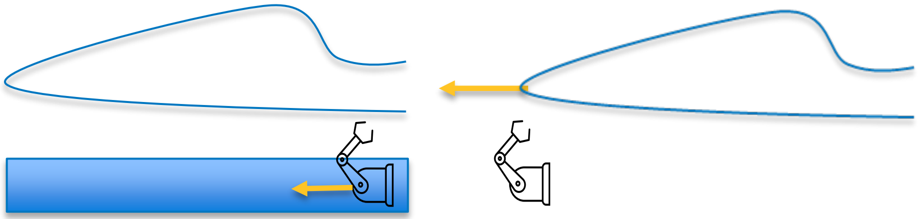

Full-Length Track With Stationary Blade	Mobile Blade With Stationary Robot
+Requires less factory space +Simple concept −High track cost −Less flexibility	+Low cost +Efficient moving-line layout +High flexibility −Complex control −Requires 2× blade length for finishing bay

How does this robot reach the entire surface?

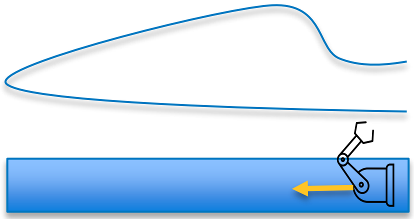

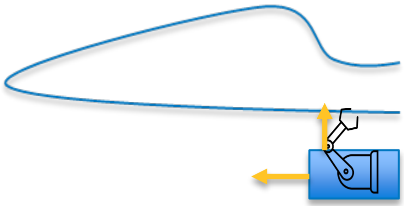

Full-Length Track With Stationary Blade	Mobile Blade With Stationary Robot	Robot on Mobile Platform
+Requires less factory space +Simple concept −High track cost −Less flexibility	+Low cost +Efficient moving-line layout +High flexibility −Complex control −Requires 2× blade length for finishing bay	+Requires less factory space +Highly flexible −Expensive automated guided vehicle (AGV) −Complex cable management −Complex control

How does this robot reach the entire surface?

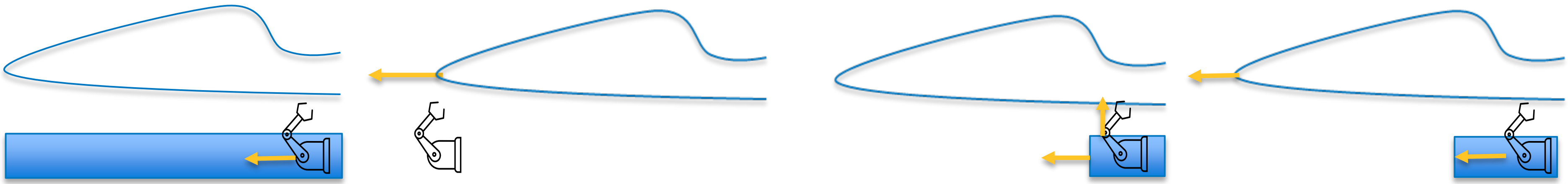

Full-Length Track With Stationary Blade

+Requires less factory space
+Simple concept
−High track cost
−Less flexibility

Mobile Blade With Stationary Robot

+Low cost
+Efficient moving-line layout
+High flexibility
−Complex control
−Requires 2× blade length for finishing bay

Robot on Mobile Platform

+Requires less factory space
+Highly flexible
−Expensive automated guided vehicle (AGV)
−Complex cable management
−Complex control

Partial-Length Track With Mobile Blade

+Lowest risk due to simplicity
+Low cost
+High flexibility
−Requires 2× blade length for finishing bay

Selecting a mobility design is critical for economic success

- Factory mobility is the main driver for capital costs and risk

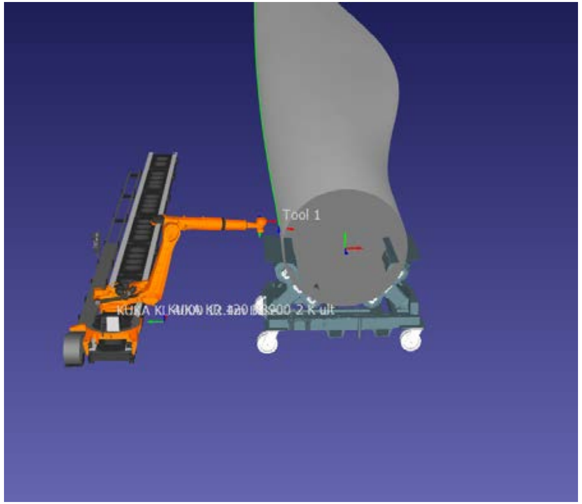

Photo by Hunter Huth, NREL

Selecting a mobility design is critical for economic success

- Factory mobility is the main driver for capital costs and risk
- Different factories have different constraints
  - Not a one-size-fits-all scenario

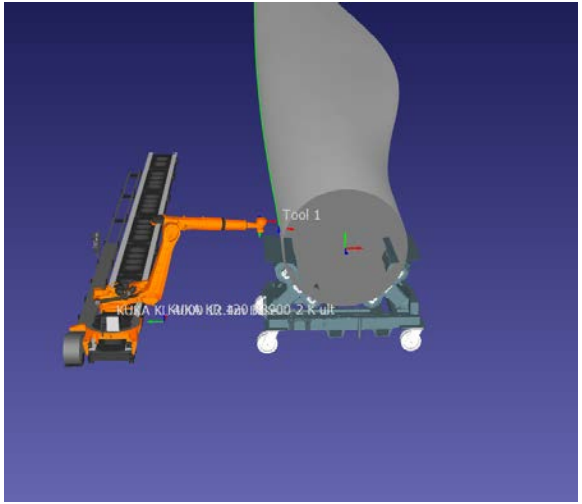

Photo by Hunter Huth, NREL

Selecting a mobility design is critical for economic success

- Factory mobility is the main driver for capital costs and risk
- Different factories have different constraints
  - Not a one-size-fits-all scenario
- Determines how adaptable this system is to new blade designs

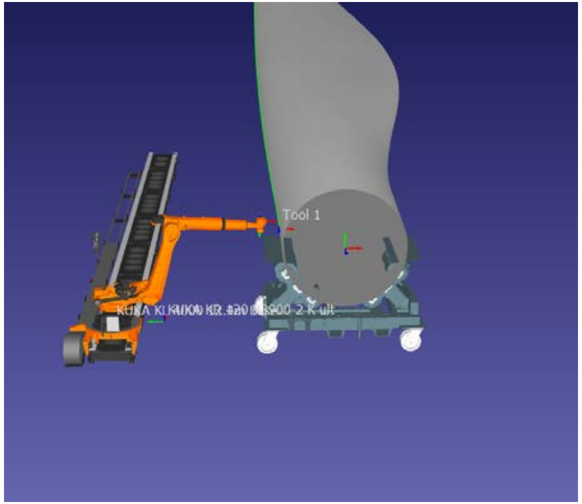

Photo by Hunter Huth, NREL

Selecting a mobility design is critical for economic success

- Factory mobility is the main driver for capital costs and risk
- Different factories have different constraints
  - Not a one-size-fits-all scenario
- Determines how adaptable this system is to new blade designs

- For this research to maximize industry impact, the rest of the system must be agnostic to mobility concept and blade design.

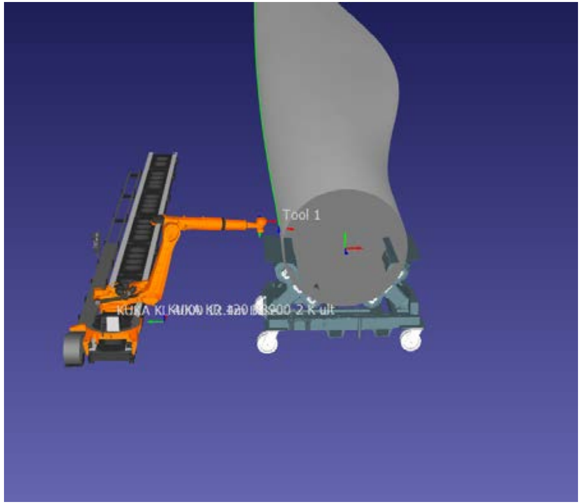

Photo by Hunter Huth, NREL

Real-time control must accompany all factory mobility concepts

- The six degrees-of-freedom of the robot arm react to the changing position of the blade
- The external motion of the blade, track, or autonomous vehicle move the robot arm along the blade.

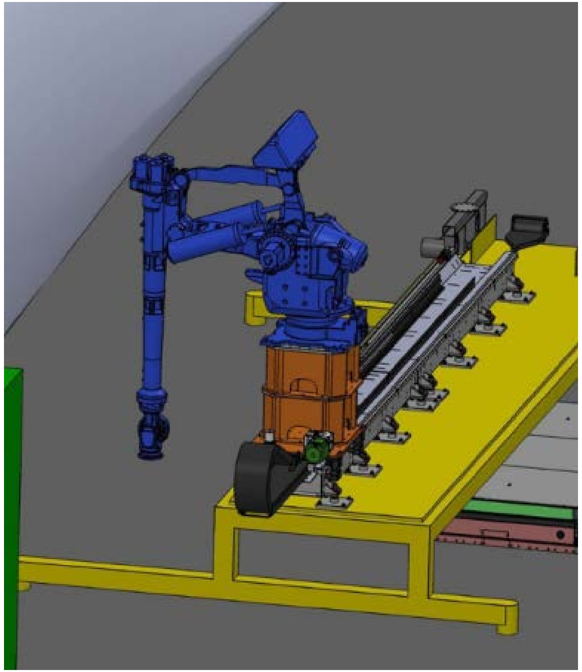

Photo by Casey Nichols, NREL

Concluding Remarks

- Automated wind blade finishing can have a large impact on blade manufacturing in the short- and mid-term

Concluding Remarks

- Automated wind blade finishing can have a large impact on blade manufacturing in the short- and mid-term
- Custom tools for robotic manufacturing allow for improved processing speeds

Concluding Remarks

- Automated wind blade finishing can have a large impact on blade manufacturing in the short- and mid-term
- Custom tools for robotic manufacturing allow for improved processing speeds
- Captured data from the blade surface can be used to produce toolpaths for automated wind blade finishing

Concluding Remarks

- Automated wind blade finishing can have a large impact on blade manufacturing in the short- and mid-term
- Custom tools for robotic manufacturing allow for improved processing speeds
- Captured data from the blade surface can be used to produce toolpaths for automated wind blade finishing
- Real-time control can optimize speed and accuracy to make automated wind blade finishing economically viable.

Acknowledgments

- LM Wind Power at GE Vernova
- Colorado Office of Economic Development and International Trade (OEDIT)
- U.S. Department of Energy (DOE) Advanced Materials and Manufacturing Technologies Office (AMMTO)
- Institute for Advanced Composites Manufacturing Innovation (IACMI)

References

Shields, Matt, Jeremy Stefek, Frank Oteri, Matilda Kreider, Elizabeth Gill, Sabina Maniak, Ross Gould, Courtney Malvik, Sam Tirone, and Eric Hines. 2023. *A Supply Chain Road Map for Offshore Wind Energy in the United States*. Golden, CO: National Renewable Energy Laboratory. NREL/TP-5000-84710. https://www.osti.gov/servlets/purl/1922189/.

Bortolotti, P., D. Berry, R. Murray, E. Gaertner, D. Jenne, R. Damiani, G. Barter, and K. Dykes. 2019. *A Detailed Wind Turbine Blade Cost Model*. Golden, CO: National Renewable Energy Laboratory. NREL/TP-5000-73585. https://www.nrel.gov/docs/fy19osti/73585.pdf.

PushCorp. 2020. “Leader in Force Compliance, Spindles, and Automation Equipment.” Accessed Oct. 14, 2023. https://pushcorp.com/.

Tyrolit. 2024. “TYROLIT POWER Surface Sander.” Accessed Aug. 26, 2024. https://www.tyrolit.com/en-us/products/tyrolit-power-surface-sander-8468/.

Huth, Hunter, Casey Nichols, Scott Lambert, Petr Sindler, Derek Berry, David Barnes, Ryan Beach, Sahand Sabet, and David Snowberg. 2024. ”Toolpath Generation for Automated Wind Turbine Blade Finishing Operations.” *Wind Energy* 27 (8): 816–826. https://doi.org/10.1002/we.2913.

Rusu, Radu Bogdan, and Steve Cousins. 2011. “3D is Here: Point Cloud Library (PCL).” Presented at IEEE International Conference on Robotics and Automation, Shanghai, China. https://doi.org/10.1109/ICRA.2011.5980567.

ZIVID. 2023. “See more. Do more. Zivid 2 industrial 3D camera.” Accessed Oct. 14, 2023. https://www.zivid.com/zivid-2.

Macenski, Steven, Tully Foote, Brian Gerkey, Chris Lalancette, and William Woodall. 2022. “Robot Operating System 2: Design, Architecture, and Uses in the Wild.” *Science Robotics* 7 (66): eabm6074. https://doi.org/10.1126/scirobotics.abm6074.

Thank You

www.nrel.gov

NREL/PR-5000-91111

This work was authored by the National Renewable Energy Laboratory, operated by Alliance for Sustainable Energy, LLC, for the U.S. Department of Energy (DOE) under Contract No. DE-AC36-08GO28308. Funding provided by the U.S. Department of Energy Advanced Materials and Manufacturing Technologies Office, Institute for Advanced Composites Manufacturing Innovation, and Colorado Office of Economic Development and International Trade.

NREL

Transforming ENERGY